

Article

# 5-Hydroxymethylfurfural Hydrodeoxygenation to 2,5-Dimethylfuran in Continuous-Flow System over Ni on Nitrogen-Doped Carbon

Francesco Brandi <sup>1,2</sup>, Marius Bäümel <sup>1</sup>, Irina Shekova <sup>1</sup>, Valerio Molinari <sup>1</sup> and Majd Al-Naji <sup>1,\*</sup> 

<sup>1</sup> Department of Colloid Chemistry, Max Plank Institute of Colloids and Interfaces, Am Mühlberg 1, 14476 Potsdam, Germany; francesco.brandi@mpikg.mpg.de (F.B.); marius.bauemel@mpikg.mpg.de (M.B.); Irina.shekova@mpikg.mpg.de (I.S.); Valerio.molinari@mpikg.mpg.de (V.M.)

<sup>2</sup> Dipartimento di Chimica Ugo Schiff, Università degli Studi di Firenze, via della Lastruccia 3, 50019 Florence, Italy

\* Correspondence: majd.al-naji@mpikg.mpg.de

Received: 30 July 2020; Accepted: 17 August 2020; Published: 19 August 2020



**Abstract:** Waste lignocellulosic biomass is sustainable and an alternative feedstock to fossil resources. Among the lignocellulosic derived compounds, 2,5-dimethylfuran (DMF) is a promising building block for chemicals, e.g., *p*-xylene, and a valuable biofuel. DMF can be obtained from 5-hydroxymethylfurfural (HMF) via catalytic deoxygenation using non-noble metals such as Ni in the presence of H<sub>2</sub>. Herein, we present the synthesis of DMF from HMF using 35 wt.% Ni on nitrogen-doped carbon pellets (35Ni/NDC) as a catalyst in a continuous flow system. The conversion of HMF to DMF was studied at different hydrogen pressures, reaction temperatures, and space times. At the best reaction conditions, i.e., 423 K, 8.0 MPa, and space time 6.4 kg<sub>Ni</sub> h kg<sub>HMF</sub><sup>-1</sup>, the 35Ni/NDC catalyst exhibited high catalytic activity with HMF conversion of 99 mol% and 80 mol% of DMF. These findings can potentially contribute to the transition toward the production of sustainable fine chemicals and liquid transportation fuels.

**Keywords:** biomass; 5-hydroxymethylfurfural; 2,5-dimethylfuran; nitrogen-doped carbon; continuous flow system; nickel

## 1. Introduction

Nowadays, crude oil is the principal raw material for the production of chemicals and fuels. However, the extensive use of this resource in the last century led to major environmental issues [1]. In the last years, it raised the need for more sustainable feedstock for energy and materials, which has to meet the growing demand for goods [2]. For these reasons, the search for a sustainable alternative to crude oil represents one of the major challenges for scientists [3].

As sustainable feedstock, lignocellulosic biomass (LCB) represents a promising candidate to replace fossil resources for fuels and chemicals [4–14]. LCB represents the most abundant biopolymer, as well as the biggest carbon reservoir in the world. In addition, LCB is worldwide and it is virtually inexhaustible [15,16]. LCB consists of three main components, i.e., cellulose (30–40%), hemicellulose (10–20%), and lignin (20–30%). Among them, hexose and pentose sugars are the main components of cellulose and hemicellulose, which correspond to about 80% of the whole biomass [4]. Although marginal, LCB is already available on a megaton (Mton) scale per year as a waste co-product from a wide series of established industrial processes, such as agroforestry and pulp processes [17,18].

In recent years, a class of sugar derived compounds such as furans have been highlighted due to their great potential for upgrading [19,20]. Among these furans, 5-hydroxymethylfuran (HMF) has great potential due to its particular chemical properties since it simultaneously has an alcohol,

an aldehyde, and a furan ring. Therefore, HMF can be easily upgraded either via an oxidative pathway, e.g., to 2,5-diformylfuran [21] or 2,5-furandicarboxylic acid [21,22], or either with reductive steps, e.g., to 2,5-tetrahydrofuran or 2,5-dimethylfuran (DMF) [23,24]. Recently, DMF production from HMF has more interest because of the great potential of DMF in several applications. As such, DMF can be considered as a high-value biofuel: when compared to bio-ethanol, DMF has a higher octane number (119 and 110, respectively), and 40% higher energy density (31 and 21 MJ L<sup>-1</sup>), this energy density is even comparable to gasoline and diesel (~35 MJ L<sup>-1</sup>) [25–27]. Additionally, DMF showed good compatibility with the already existing spark-ignition engines, which potentially allows it to be used immediately as fuel [28]. Despite its potential as a fuel, DMF is already used as a solvent in the cosmetic and pharmaceutical industries [27]. Moreover, DMF can also be further upgraded to produce *p*-xylene, which is the main industrial precursor for PET [29,30].

In 2007, Román-Leshkov et al., pioneered the HMF hydrodeoxygenation to DMF in a batch system, using a bimetallic Ru-Cu/C, yielding in 71 mol% of DMF at 493 K in *n*-butanol [23]. Also, a series of noble metal has been efficiently used for the same purpose, such as Pd, Ru, Pt, and Rh supported on C [27,31]. Although, very active noble metal has an intrinsically high cost, which has pushed researchers to find alternatives, such as non-noble metal. In this regard, Ni and Cu have been efficiently used in the DMF production from HMF. For instance, Yang et al. reported a DMF yield of 95 mol% using a Ni-Co bimetallic catalyst supported on carbon, in batch systems at 403 K and 1 MPa of H<sub>2</sub> [32]. Similarly, Han et al. obtained 95 mol% using a bimetallic alloy of Ni and Mo deposited on mesoporous MoS<sub>2</sub>/mAl<sub>2</sub>O<sub>3</sub> at 403 K and 1 MPa of H<sub>2</sub> [33]. Moreover, Bordoloi and coworkers demonstrated the synergic effect of using Ni on nitrogen-doped carbon, yielding in almost complete conversion of HMF to DMF at 423 K [34]. All these studies that represented a high HMF conversion and DMF yield were conducted in batch systems.

When compared to batch, flow chemistry allows more efficient heat transfer, as well as less hazardous systems, and decreases the downstream costs [35,36]. For these reasons, in 2019, the International Union of Pure and Applied Chemistry (IUPAC) mentioned flow chemistry among the 10 chemical innovations with the potential to make our planet more sustainable [37]. Regarding DMF production from HMF in flow systems, to date, few investigations have been reported. Uniquely, Braun and Antonietti [25] reported a cascade-flow reactor for DMF production starting from fructose, combining solid acid-catalyst (Amberlyst 15) with an Ni catalyst on a tungsten-carbide support with DMF yield of 39 mol% at 373 K. Using HMF as a precursor, Luo et al. [31], reported a relatively low DMF yield of 40 mol% using Ni on C in flow systems. Similarly, Luo et al. founded the almost complete conversion of HMF to DMF over a nanocrystalline Ni-Cu alloy deposited on the carbon support.

In general, the current state-of-the-art HMF conversion to DMF indicates that high yields are possible even with non-noble metals [16]. However, these works are conducted in a batch system and use a catalyst in powder form on an mg-scale. To speed up the transition from fossil fuel toward a sustainable society, we believe is necessary to synthesize and use a scalable catalyst. Therefore, in this work, we report on the use of 35 wt.% Ni on nitrogen-doped carbon, which has been synthesized according to our previously reported “kitchen lab” approach [38]. The performance of this catalyst in the hydrodeoxygenation of HMF to DMF in ethanol using continuous-flow systems was assessed.

## 2. Experimental Methods

### 2.1. Materials

D-glucose anhydrous (99%), urea (99%), and 5-methylfurfural (99%) were purchased from Sigma-Aldrich. ZnO nanoparticles (average diameter = 20 nm) were ordered from Nanostructures and Amorphous. 2,5-bis-hydroxymethylfuran (95%) was supplied by Oxchem. Semolina was purchased from the brand Divella (durum wheat type). Absolute ethanol (HPLC grade, 99.9%) and hydrochloric acid (1 M in H<sub>2</sub>O) were supplied from VWR. Toronto Research Chemicals provided 5-hydroxymethylfurfural (99%). Nickel (II) nitrate hexahydrate (99%) was acquired from Roth.

Acros Organics provided 2,5-dimethylfuran (99%) and 5-methylfurfuryl alcohol. All chemicals were used as received without any further purification.

## 2.2. Catalyst Preparation

The pellet-shaped 35 wt.% Ni on the nitrogen-doped carbon (35Ni/NDC) was prepared following the “kitchen-lab” approach previously reported by our group [38]. The synthesis consisted of a three-step process: extrusion of carbon-pellet precursor, carbonization, and Ni nanoparticle deposition. For the synthetic details, we refer to our recent publication [38].

## 2.3. Catalyst Characterization

The fresh 35 wt.% Ni on nitrogen-doped carbon (35Ni/NDC) was characterized using inductively elemental analysis, N<sub>2</sub> physisorption, powder X-ray diffraction (XRD), thermogravimetric analysis (TGA), transmission electron microscopy (TEM), and temperature-programmed desorption of ammonia (NH<sub>3</sub>-TPD). The description of the applied procedures is reported in detail in the Electronic Supporting Information (ESI).

## 2.4. Catalytic Experiments

The 5-hydroxymethylfurfural (HMF) hydrodeoxygenation experiments were conducted in a homemade continuous-flow system (Figures S1 and S2 at ESI), using a fixed bed reactor, similarly to our previously described setup [12,38]. This system is composed of: (1) HPLC pump equipped with a pressure sensor (Knauer Azura P 4.1S Series), (2) a two-sided opened heating unit equipped with heating mantle (Figure S2 at ESI) and heat controller (Model # 4848 from Parr Instrument Company), (3) mass flow controller to supply H<sub>2</sub> (Brook Instruments SLA5800) connected to the with a T-union for the gas-liquid mixer (Swagelok SS-400-30), (4) sampling unit equipped with proportional relief valves as a pressure regulator (Swagelok SS-RLM4M8F8-EP), cf. Figure S1 in the section two “continuous flow setup” at ESI. All the used tubing in this setup was made of stainless steel and provided by Swagelok.

In a typical experiment, an ethanol solution of HMF (0.05 M) was fed at different flow rates, i.e., 0.30 cm<sup>3</sup> min<sup>-1</sup> using the HPLC pump. Therefore, the educts were mixed with an excess of H<sub>2</sub> (Q<sub>H<sub>2</sub></sub> = 12 cm<sup>3</sup> min<sup>-1</sup>). Prior to being in contact with the catalyst, the solution was pre-heated through the pre-heating unit to ensure an isothermal heat distribution over the catalyst bed. A 1.0 g quantity of catalyst pellets were placed in the fixed bed reactor between 0.1 g of quartz wool. The reactor temperature and pressure were kept at room temperature for almost 15 min, later the system pressure was adjusted to the targeted values of pressure and temperature, i.e., 2.0, 5.0, and 8.0 MPa and 373, 398, and 423 K, respectively. Once a steady-state was reached (after 45 min of starting feeding the reaction solution), a sample (ca. 1.0 cm<sup>3</sup>) was collected.

Reactant and product identification and quantification were performed using gas chromatography equipped with a mass spectrometer detector (GC-MS) and with a flame ionization detector (GC-FID). The detailed information about the reactants and product quantification, as well as the kinetic investigation, can be found at the ESI.

## 3. Result and Discussion

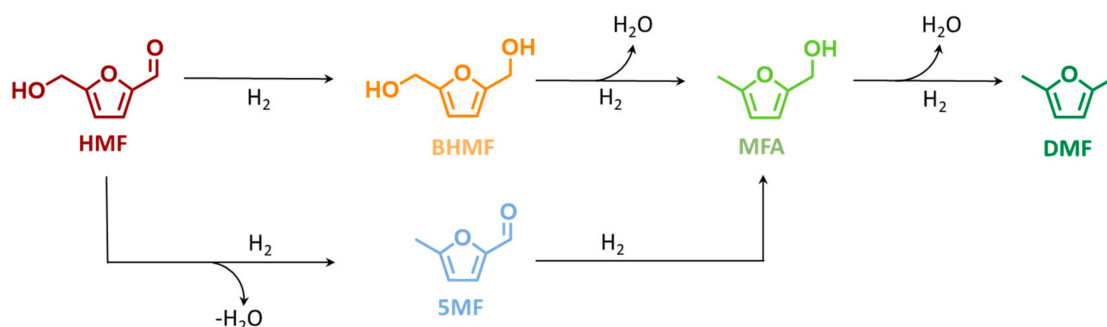
The 35 wt.% nickel on nitrogen-doped carbon (35Ni/NDC) was synthesized following the “kitchen lab” approach [38]. The textural properties of the prepared 35Ni/NDC catalyst are reported in Table 1 and Figures S3 and S4 of the Electronic Supporting Information (ESI). As expected, the carbonized precursor exhibited a high specific surface area (755 m<sup>2</sup> g<sup>-1</sup>), as well as a relatively high N content (C/N ratio of 22), cf., Table 1 and Figure S3 of the ESI. Therefore, 35 wt.% of Ni nanoparticles have been introduced via wet impregnation and the reduction-calcination process. As expected, the introduction of Ni nanoparticles yielded in a slightly reduced surface area, from 755 to 578 m<sup>2</sup> g<sup>-1</sup>. Moreover, the XRD reflections pattern showed the typical turbostratic carbon broad peak at 2θ of 25°, as well as the

typical Ni<sup>0</sup> reflections at 44° and 51°, viz., Figure S4 in the ESI. The TEM pictures also showed the presence of Ni nanoparticles of the expected size, i.e., 20–40 nm, c.f. Figure S5 at the ESI.

**Table 1.** Textural properties and chemical composition of NDC and 35Ni/NDC obtained with N<sub>2</sub> physisorption and EA-ICP.

Catalyst	C/wt.%	N/wt.%	C/N Ratio	Ni/wt.%	A <sub>BET</sub> /m <sup>2</sup> g <sup>-1</sup>
NDC	75	3.7	22	-	755
35Ni/NDC	55	2.8	20	34.7	578

The catalytic activity of the prepared 35Ni/NDC pellets catalyst has been studied for the catalytic hydrodeoxygenation of 5-hydroxymethylfurfural (HMF) toward 2,5-dimethylfuran (DMF) in the above described continuous flow system, c.f. Scheme 1. To investigate the optimal reaction conditions that lead to achieving a high yield of DMF from HMF, the reaction temperature, H<sub>2</sub> pressure, and space time have been varied. Initially, the effect of temperature was studied at three different temperatures, i.e., 373, 398, and 423 K, cf. Figure 1. Interestingly at 373 K and using 35Ni/NDC, a high HMF conversion (72 mol%) was found. Despite the high HMF conversion, DMF yield was observed to be only 1.3 mol%, combined with 5-methylfurfuryl alcohol (MFA) in a yield of 3.0 mol%, 2,5-bis-hydroxymethylfuran (BHMF) yield of 4.8 mol% and a 5-methylfurfural (5-MF) yield in trace (<1 mol%). This high HMF conversion is due to the etherification of HMF to 5-(ethoxymethyl)furfural and the formation of the respective acetal (2-(diethoxymethyl)furan-2-yl)-methanol), as well as partial degradation of HMF. All these side products were identified via GC-MS [39]. For the deep understanding of this observation, a comparison of an experiment in the absence of catalyst and with only the support (NDC) was applied viz. in Figure S6 in the ESI. In contrast, in the absence of catalyst, i.e., either NDC or 35Ni/NDC, and at 373, 398, and 423 K, very low HMF conversion was detected, i.e., 0, 6.1, and 16 mol%, respectively. In addition, at these three reaction temperatures and in the absence of a catalyst, no etherification products were detected. Differently, the experiment with NDC exhibited a high HMF conversion of 61, 66, and 94 mol% at 373, 398, and 423 K, respectively. This is due to the presence of active acid sites at the support material proved via NH<sub>3</sub>-TPD, viz. Figure S7 at ESI. These acid sites could promote the HMF etherification process [40]. This finding is in accordance with previous studies on HMF etherification using alcohols, such as ethanol, which yielded to a high etherification rate even at low temperatures in the presence of Brønsted and Lewis acidic sites [40–42]. Moreover, at 423 K in the presence of only NDC, an unexpected 10 mol% of Y<sub>DMF</sub> was detected. This finding could be explained by catalytic activity either of Zn impurities of the NDC or the reactor wall metal impurities in combination with the high surface area of the NDC pellets. Despite high HMF conversion, the hydrodeoxygenation products, i.e., DMF, BHMF, MFA, and 5-MF, at 373 K were found in a low amount <5 mol%. Increasing the reaction temperature from 373 to 398 K corresponded to high HMF conversion (92 mol%) and an increase in yield of BHMF, (from 4.8 to 17 mol%), MFA (from 2.3 to 3.2 mol%) and DMF (from 1.3 to 12 mol%). At the same time, 5-MF was found constantly in traces below 1 mol%. Additionally, a further temperature increase from 398 to 423 K, led to a HMF conversion (98 mol%) and higher DMF yield (from 12 to 69 mol%), whereas the intermediates BHMF and MFA dropped from 17 to 6.0 mol% and from 3.2 to 0.4 mol%, respectively.



**Scheme 1.** Proposed hydrodeoxygenation pathway of 5-hydroxymethylfurfural (HMF) to 5-methylfurfuryl alcohol (MFA) and to 2,5-dimethylfuran (DMF), via 2,4-bis-hydroxymethylfuran (BHMF) or 5-methylfurfural (5-MF).

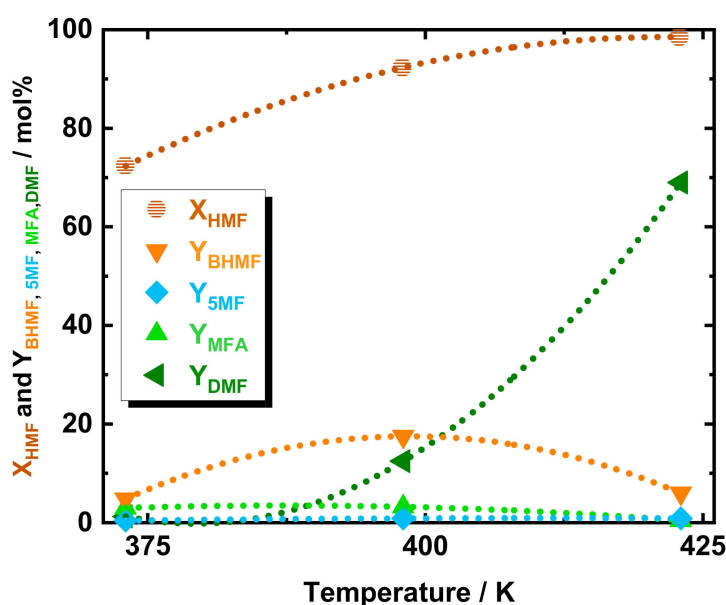


**Figure 1.** The conversion of HMF and yield of DMF, BHMF, 5-MF, and MFA as a function of temperature. Reaction conditions:  $c_{\text{HMF}} = 0.05 \text{ M}$ ,  $Q_{\text{educt}} = 0.3 \text{ cm}^3 \text{ min}^{-1}$ , i.e., space time =  $3.2 \text{ kg}_{\text{Ni}} \text{ h kg}_{\text{HMF}}^{-1}$ ,  $T = 373, 398, \text{ and } 423 \text{ K}$ ,  $P_{\text{system}} = 8.0 \text{ MPa}$ ,  $\text{H}_2 \text{ flow} = 12 \text{ cm}^3 \text{ min}^{-1}$ ,  $m_{\text{catalyst}} = 1.2 \text{ g}$ .

Due to the higher DMF yield (69 mol%), 423 K was selected as the optimized temperature for further investigation. No further increase at the reaction temperature was applied to avoid HMF polymerization, i.e., humification. Generally, among the two possible first step intermediates, see Scheme 1, this temperature study indicates BHMF as the most present intermediate while 5-MF was found only in traces. The poor 5-MF yield (<1 mol%) combined with BHMF as a predominant intermediate gives an indication of the preferable kinetic pathway. Therefore, it can be deduced that the reaction proceeds primarily via reduction of the HMF aldehydic function to BHMF, followed by two consecutive hydrodeoxygenation to MFA and DMF, viz. Scheme 1. The apparent activation energy ( $E_a$ ) of DMF formation has been extrapolated from the Arrhenius plot assuming a zeroth-order reaction (Figure S8 at the ESI). Accordingly,  $E_a$  was found at  $71 \text{ kJ mol}^{-1}$ , which is in good agreement with the value reported in the literature of  $64 \text{ kJ mol}^{-1}$  using Ni on carbon but in a batch system. The good agreement between the batch and flow experiments is a good indication that the HMF hydrodeoxygenation to DMF is not diffusion-limited.

To investigate the effect of pressure in DMF yield, c.f. Scheme 1, a variation of H<sub>2</sub> pressure from 2.0 to 5.0 MPa and to 8.0 MPa was applied at 423 K, viz. in Figure 2. As expected, the conversion of HMF was found independent from the pressure, with a value always above 95 mol% in the selected

range of pressure. Increasing the pressure from 2.0 to 4.0 MPa and to 8.0 MPa led to an increase in DMF yield from 33 to 58 mol% and to 69 mol%, respectively. At 2.0 MPa, the  $Y_{\text{DMF}}$  decrease corresponded a higher yield of the intermediate, with  $Y_{\text{BHMF}}$ ,  $Y_{\text{MFA}}$ , and  $Y_{\text{5MF}}$  increasing to 33, 6.5, and 1.0 mol%, respectively. Similarly to the aforementioned temperature study, the BHMF was found to be the predominant intermediate, which emphasized that the preferable pathway for DMF is via BHMF—c.f. Scheme 1.

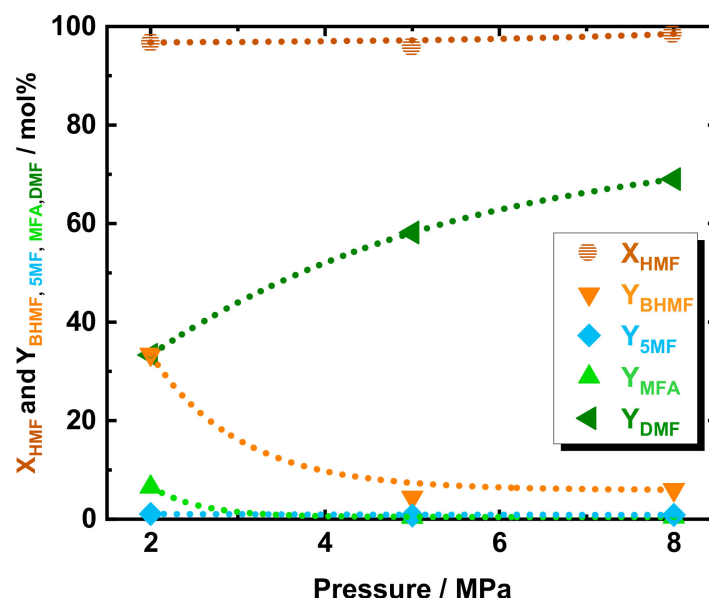


**Figure 2.** The conversion of HMF and yield of DMF, BHMF, 5-MF, and MFA as a function of system pressure over 35Ni/NDC. Reaction conditions:  $c_{\text{HMF}} = 0.05 \text{ M}$ ,  $Q_{\text{educt}} = 0.3 \text{ cm}^3 \text{ min}^{-1}$ , i.e., space time =  $3.2 \text{ kg}_{\text{Ni}} \text{ h kg}_{\text{HMF}}^{-1}$ ,  $T = 423 \text{ K}$ ,  $P_{\text{system}} = 2.0, 5.0, \text{ and } 8.0 \text{ MPa}$ ,  $\text{H}_2 \text{ flow} = 12 \text{ cm}^3 \text{ min}^{-1}$ ,  $m_{\text{catalyst}} = 1.2 \text{ g}$ .

The influence of space time on the DMF yield was assessed. For this purpose, the educts flow was varied from 0.15 to 0.3 to 0.6 and  $1.0 \text{ cm}^3 \text{ min}^{-1}$ , which corresponds to a space time of 6.4, 3.2, 1.6, and  $0.95 \text{ kg}_{\text{Ni}} \text{ h kg}_{\text{HMF}}^{-1}$ , respectively, c.f. Figure 3. At high space time, such as of 6.4, 3.2, and  $1.6 \text{ kg}_{\text{Ni}} \text{ h kg}_{\text{HMF}}^{-1}$  the conversion of HMF was found to be above 95 mol%, while at fast flow the conversion dropped to 68 mol%. Also, the  $Y_{\text{DMF}}$  showed a strong dependence on space time, increasing from 8.9 to 41 to 69 mol% and subsequently to 80 mol% in correspondence with space time increasing from 0.95 to 1.6 to 6.4 and to  $3.2 \text{ kg}_{\text{Ni}} \text{ h kg}_{\text{HMF}}^{-1}$ , respectively. In contrast, the intermediates alcohol yield, i.e.,  $Y_{\text{BHMF}}$  and  $Y_{\text{MFA}}$ , exhibited inverse dependence to space time. Particularly, BHMF was found to be the major product at the lowest space time with a  $Y_{\text{BHMF}}$  of 26 mol% at  $0.95 \text{ kg}_{\text{Ni}} \text{ h kg}_{\text{HMF}}^{-1}$ . In addition, an increase in space time to 1.6 and  $3.2 \text{ kg}_{\text{Ni}} \text{ h kg}_{\text{HMF}}^{-1}$  showed a decrease of  $Y_{\text{BHMF}}$  to 13 and 4.8 mol%, respectively. Similarly, MFA exhibited a relatively high  $Y_{\text{MFA}}$  of 6.4 mol% at  $0.95 \text{ kg}_{\text{Ni}} \text{ h kg}_{\text{HMF}}^{-1}$ , whereas MFA yield dropped to below 3 mol% by increasing the space time to 1.6 and  $3.2 \text{ kg}_{\text{Ni}} \text{ h kg}_{\text{HMF}}^{-1}$ . Finally, the TGA of the spent 35Ni/NDC catalyst after five hours of reaction showed a minimal mass loss (<10 wt.%) before 750 K, indicating minimal product deposition on top of the catalyst (Figure S9 of the ESI).

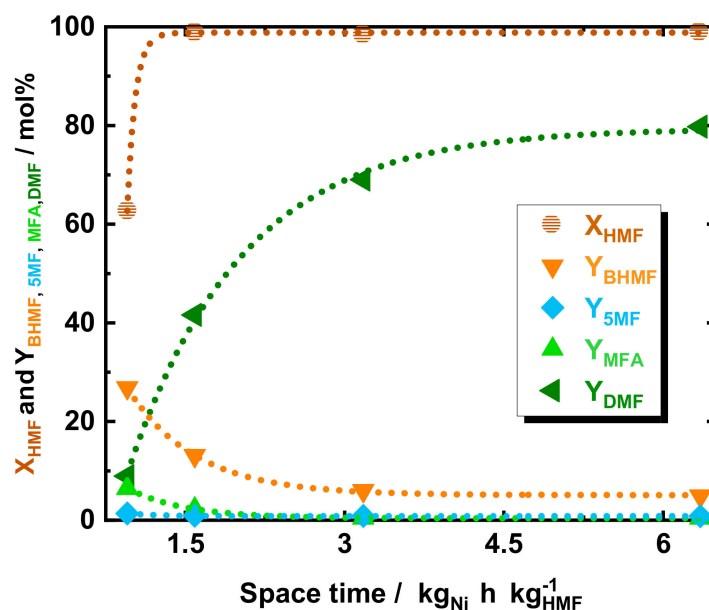


**Figure 3.** The conversion of HMF and yield of DMF, BHMF, 5-MF, and MFA as a function of space time using 35Ni/NDC. Reaction conditions:  $c_{\text{HMF}} = 0.05 \text{ M}$ ,  $Q_{\text{educt}} = 0.15, 0.3, 0.6,$  and  $1.0 \text{ cm}^3 \text{ min}^{-1}$ , i.e., space time = 6.4, 3.2, 1.6, and  $0.95 \text{ kg}_{\text{Ni}} \text{ h kg}_{\text{HMF}}^{-1}$ ,  $T = 423 \text{ K}$ ,  $P_{\text{system}} = 8.0 \text{ MPa}$ ,  $\text{H}_2$  flow =  $12 \text{ cm}^3 \text{ min}^{-1}$   $m_{\text{catalyst}} = 1.2 \text{ g}$ .

#### 4. Conclusions

The 35Ni/NDC pellets exhibited high catalytic performances in the continuous flow hydrodeoxygenation of 5-hydroxymethylfurfural to 2,5-dimethylfuran. The presence of Ni was found essential to give a high yield of DMF, i.e.,  $Y_{\text{DMF}}$  of 80 mol% at 423 K, 8.0 MPa and  $6.4 \text{ kg}_{\text{Ni}} \text{ h kg}_{\text{HMF}}^{-1}$ . In addition, high  $\text{H}_2$  pressure has been found to be essential for an efficient DMF production from lignocellulosic derivable HMF. The studies conducted at low space time and low temperature indicated that the reaction pathway for DMF synthesis from HMF is preferably proceeded via 2,5-bis-hydroxymethylfuran (BHMF) instead of the 5-methylfurfural (5-MF) route. We believe that more focus on the use of heterogeneous catalysts in a continuous-flow system for biomass valorization has the potential to speed up the transition toward more sustainable production of fine chemicals and liquid transportation fuels, and as a consequence to a more sustainable society.

**Supplementary Materials:** The following are available online at <http://www.mdpi.com/2673-4079/1/2/9/s1>, Figure S1: The setup for the continuous flow hydrodeoxygenation of 5-Hydroxymethylfurfural (HMF) to 2,5-Dimethylfuran (DMF), consisting of (1) HPLC pump equipped with pressure control, (2) heating unit (its section can be viz. at Figure S2, (3) Mass-flow controller for  $\text{H}_2$  supply and (4) sampling unit with proportional relief valve. Figure S2: Homemade aluminum heating block used to ensure efficient heating, consisting of three location holes: (1) fixed bed reactor place (2) thermocouple location for temperature control and (3) pre-heating unit. Figure S3:  $\text{N}_2$ -physisorption isotherms of the NDC and 35Ni/NDC. Figure S4: XRD pattern of 35Ni/NDC. The symbols indicate the typical reflection for  $\text{Ni}_0$  and C present in literature. Figure S5: TEM image for 35Ni/NDC. Figure S6: The conversion of HMF and yield of DMF in presence of only NDC and without catalyst as a function of temperature. Reaction conditions:  $c_{\text{HMF}} = 0.05 \text{ M}$ ,  $Q_{\text{educt}} = 0.3 \text{ cm}^3 \text{ min}^{-1}$ , i.e., space time =  $3.2 \text{ kg}_{\text{Ni}} \text{ h kg}_{\text{HMF}}^{-1}$ ,  $T = 373 \text{ K}, 398 \text{ K}$  and  $423 \text{ K}$ ,  $P_{\text{system}} = 8.0 \text{ MPa}$ ,  $\text{H}_2$  flow =  $12 \text{ cm}^3 \text{ min}^{-1}$   $m_{\text{catalyst}} = 0.78 \text{ g}$ . and  $0 \text{ g}$ . Figure S7:  $\text{NH}_3$ -TPD of NDC (black line) and 35Ni/NDC (blue line). Figure S8: Arrhenius plot for the DMF production from HMF over 35Ni/NDC at different reaction temperatures, i.e., 323 K, 398 K and 423 K. Figure S9: TGA curve of the spent 35Ni/NDC.

**Author Contributions:** F.B. has conducted the experiments, prepared and wrote the draft of the manuscript, M.B. I.S. and V.M. have reviewed and edited the manuscript. M.A.-N. supervised the work and edited the final version. Of the manuscript. All authors have read and agreed to the published version of the manuscript.

**Funding:** This research received no external funding.

**Acknowledgments:** The authors are grateful for the financial support from Max Planck, Society, Unifying System in Catalysis “UniSysCat” Cluster of Excellence Berlin-Potsdam. Francesco Brandi greatly acknowledges the ERASMUS+ project for the financial support of the traineeship at the Max Planck Institute of Colloids and Interfaces. Thanks are also extended to Jessica Brandt, and Heike Runge from Max Planck Institute of Colloids and Interfaces for ICP-OES, and SEM and TEM measurements, respectively. The effort of the Electrical and Mechanical Workshops at the Max Planck Institute of Colloids and Interfaces is greatly acknowledged.

**Conflicts of Interest:** The authors declare no conflict of interest.

## References

1. Ravishankara, A.R.; Rudich, Y.; Pyle, J.A. Role of Chemistry in Earth’s Climate. *Chem. Rev.* **2015**, *115*, 3679–3681. [CrossRef] [PubMed]
2. Schellnhuber, H.J. Why the right climate target was agreed in Paris. *Nat. Clim. Chang.* **2016**, *6*, 649–653. [CrossRef]
3. Sheldon, R.A. Metrics of Green Chemistry and Sustainability: Past, Present, and Future. *ACS Sustain. Chem. Eng.* **2017**, *6*, 32–48. [CrossRef]
4. Isikgor, F.H.; Becer, C.R. Lignocellulosic biomass: A sustainable platform for the production of bio-based chemicals and polymers. *Polym. Chem.* **2015**, *6*, 4497–4559. [CrossRef]
5. Graglia, M.; Kanna, N.; Esposito, D. Lignin Refinery: Towards the Preparation of Renewable Aromatic Building Blocks. *ChemBioEng Rev.* **2015**, *2*, 377–392. [CrossRef]
6. Sheldon, R.A. Green and sustainable manufacture of chemicals from biomass: State of the art. *Green Chem.* **2014**, *16*, 950–963. [CrossRef]
7. Zhou, C.H.; Xia, X.; Lin, C.X.; Tong, D.S.; Beltramini, J. Catalytic conversion of lignocellulosic biomass to fine chemicals and fuels. *Chem. Soc. Rev.* **2011**, *40*, 5588–5617. [CrossRef]
8. Alonso, D.M.; Bond, J.Q.; Dumesic, J.A. Catalytic conversion of biomass to biofuels. *Green Chem.* **2010**, *12*, 1493–1513. [CrossRef]
9. Liao, Y.; Koelewijn, S.-F.; van den Bossche, G.; van Aelst, J.; van den Bosch, S.; Renders, T.; Navare, K.; Nicolai, T.; van Aelst, K.; Maesen, M. A sustainable wood biorefinery for low-carbon footprint chemicals production. *Science* **2020**, *367*, 1385–1390. [CrossRef]
10. Besson, M.; Gallezot, P.; Pinel, C. Conversion of biomass into chemicals over metal catalysts. *Chem. Rev.* **2014**, *114*, 1827–1870. [CrossRef]
11. Kumru, B.; Mesa, J.M.; Antonietti, M.; Al-Naji, M. Metal-Free Visible-Light-Induced Dithiol–Ene Clicking via Carbon Nitride to Valorize 4-Pentenoic Acid as a Functional Monomer. *ACS Sustain. Chem. Eng.* **2019**, *7*, 17574–17579. [CrossRef]
12. Al-Naji, M.; Puertolas, B.; Kumru, B.; Cruz, D.; Baumel, M.; Schmidt, B.; Tarakina, N.V.; Perez-Ramirez, J. Sustainable Continuous Flow Valorization of gamma-Valerolactone with Trioxane to alpha-Methylene-gamma-Valerolactone over Basic Beta Zeolites. *Chemsuschem* **2019**, *12*, 2628–2636. [CrossRef] [PubMed]
13. Al-Naji, M.; Popova, M.; Chen, Z.; Wilde, N.; Gläser, R. Aqueous-Phase Hydrogenation of Levulinic Acid Using Formic Acid as a Sustainable Reducing Agent Over Pt Catalysts Supported on Mesoporous Zirconia. *ACS Sustain. Chem. Eng.* **2019**, *8*, 393–402. [CrossRef]
14. Al-Naji, M.; van Aelst, J.; Liao, Y.; d’Hullian, M.; Tian, Z.; Wang, C.; Gläser, R.; Sels, B.F. Pentanoic acid from gamma-valerolactone and formic acid using bifunctional catalysis. *Green Chem.* **2020**, *22*, 1171–1181. [CrossRef]
15. Corma, A.; Iborra, S.; Velty, A. Chemical routes for the transformation of biomass into chemicals. *Chem. Rev.* **2007**, *107*, 2411–2502. [CrossRef]
16. Gerardy, R.; Debecker, D.P.; Estager, J.; Luis, P.; Monbaliu, J.M. Continuous Flow Upgrading of Selected C2-C6 Platform Chemicals Derived from Biomass. *Chem. Rev.* **2020**. [CrossRef] [PubMed]
17. Environmental Paper Network. International Annual Report. 2018. Available online: <https://environmentalpaper.org/tools-and-resources/reports/> (accessed on 29 July 2020).
18. Schutyser, W.; Renders, T.; van den Bosch, S.; Koelewijn, S.F.; Beckham, G.T.; Sels, B.F. Chemicals from lignin: An interplay of lignocellulose fractionation, depolymerisation, and upgrading. *Chem. Soc. Rev.* **2018**, *47*, 852–908. [CrossRef] [PubMed]



19. Werpy, T.; Petersen, G. *Top Value Added Chemicals from Biomass: Vol.1—Results of Screening for Potential Candidates from Sugars and Synthesis Gas*; Report No. NREL/TP-510-35523; U.S. Department of Energy: Oak Ridge, TN, USA, 2004.
20. Bozell, J.J.; Petersen, G.R. Technology development for the production of biobased products from biorefinery carbohydrates—the US Department of Energy’s “Top 10” revisited. *Green Chem.* **2010**, *12*, 539–554. [[CrossRef](#)]
21. Zhang, D.; Dumont, M.-J. Advances in polymer precursors and bio-based polymers synthesized from 5-hydroxymethylfurfural. *J. Polym. Sci. Pol. Chem.* **2017**, *55*, 1478–1492. [[CrossRef](#)]
22. Esposito, D.; Antonietti, M. Redefining biorefinery: The search for unconventional building blocks for materials. *Chem. Soc. Rev.* **2015**, *44*, 5821–5835. [[CrossRef](#)]
23. Román-Leshkov, Y.; Barrett, C.J.; Liu, Z.Y.; Dumesic, J.A. Production of dimethylfuran for liquid fuels from biomass-derived carbohydrates. *Nature* **2007**, *447*, 982–985. [[CrossRef](#)] [[PubMed](#)]
24. Climent, M.J.; Corma, A.; Iborra, S. Conversion of biomass platform molecules into fuel additives and liquid hydrocarbon fuels. *Green Chem.* **2014**, *16*, 516–547. [[CrossRef](#)]
25. Braun, M.; Antonietti, M. A continuous flow process for the production of 2, 5-dimethylfuran from fructose using (non-noble metal based) heterogeneous catalysis. *Green Chem.* **2017**, *19*, 3813–3819. [[CrossRef](#)]
26. van Putten, R.J.; van der Waal, J.C.; de Jong, E.; Rasrendra, C.B.; Heeres, H.J.; de Vries, J.G. Hydroxymethylfurfural, a versatile platform chemical made from renewable resources. *Chem. Rev.* **2013**, *113*, 1499–1597. [[CrossRef](#)] [[PubMed](#)]
27. Chen, S.; Wojcieszak, R.; Dumeignil, F.; Marceau, E.; Royer, S. How Catalysts and Experimental Conditions Determine the Selective Hydroconversion of Furfural and 5-Hydroxymethylfurfural. *Chem. Rev.* **2018**, *118*, 11023–11117. [[CrossRef](#)]
28. Zhong, S.; Daniel, R.; Xu, H.; Zhang, J.; Turner, D.; Wyszynski, M.L.; Richards, P. Combustion and Emissions of 2,5-Dimethylfuran in a Direct-Injection Spark-Ignition Engine. *Energy Fuels* **2010**, *24*, 2891–2899. [[CrossRef](#)]
29. Teixeira, I.F.; Lo, B.T.; Kostetsky, P.; Stamatakis, M.; Ye, L.; Tang, C.C.; Mpourmpakis, G.; Tsang, S.C. From Biomass-Derived Furans to Aromatics with Ethanol over Zeolite. *Angew. Chem. Int. Ed.* **2016**, *55*, 13061–13066. [[CrossRef](#)]
30. Mendoza-Mesa, J.; Brandi, F.; Shekova, I.; Antonietti, M.; Al-Naji, M. *p*-xylene from 2,5-dimethylfuran and acrylic acid using zeolite in continuous flow system. *Green Chem.* **2020**. under review.
31. Luo, J.; Arroyo-Ramírez, L.; Wei, J.; Yun, H.; Murray, C.B.; Gorte, R.J. Comparison of HMF hydrodeoxygenation over different metal catalysts in a continuous flow reactor. *Appl. Catal. A Gen.* **2015**, *508*, 86–93. [[CrossRef](#)]
32. Yang, P.; Xia, Q.; Liu, X.; Wang, Y. High-yield production of 2,5-dimethylfuran from 5-hydroxymethylfurfural over carbon supported Ni–Co bimetallic catalyst. *J. Energy Chem.* **2016**, *25*, 1015–1020. [[CrossRef](#)]
33. Han, W.; Tang, M.; Li, J.; Li, X.; Wang, J.; Zhou, L.; Yang, Y.; Wang, Y.; Ge, H. Selective hydrogenolysis of 5-hydroxymethylfurfural to 2, 5-dimethylfuran catalyzed by ordered mesoporous alumina supported nickel-molybdenum sulfide catalysts. *Appl. Catal. B Environ.* **2020**, *268*, 118748. [[CrossRef](#)]
34. Goyal, R.; Sarkar, B.; Bag, A.; Siddiqui, N.; Dumbre, D.; Lucas, N.; Bhargava, S.K.; Bordoloi, A. Studies of synergy between metal–support interfaces and selective hydrogenation of HMF to DMF in water. *J. Catal.* **2016**, *340*, 248–260. [[CrossRef](#)]
35. Gérardy, R.; Morodo, R.; Estager, J.; Luis, P.; Debecker, D.P.; Monbaliu, J.-C.M. Sustaining the Transition from a Petrobased to a Biobased Chemical Industry with Flow Chemistry. *Top. Curr. Chem.* **2018**, *377*, 1.
36. Gérardy, R.; Emmanuel, N.; Toupy, T.; Kassan, V.-E.; Tshibalonza, N.N.; Schmitz, M.; Monbaliu, J.-C.M. Continuous Flow Organic Chemistry: Successes and Pitfalls at the Interface with Current Societal Challenges. *Eur. J. Org. Chem.* **2018**, *2018*, 2301–2351.
37. Gomollón-Bel, F. Ten Chemical Innovations That Will Change Our World\_ IUPAC identifies emerging technologies in Chemistry with potential to make our planet more sustainable. *Chem. Int.* **2019**, *41*, 12–17. [[CrossRef](#)]
38. Brandi, F.; Bäümel, M.; Molinari, V.; Shekova, I.; Lauer mann, I.; Heil, T.; Antonietti, M.; Al-Naji, M. Nickel on nitrogen-doped carbon pellets for continuous-flow hydrogenation of biomass-derived compounds in water. *Green Chem.* **2020**, *22*, 2755–2766. [[CrossRef](#)]
39. Bäümel, M. Upgrading of Lignocellulose-Derived Sugars to Value-Added Chemicals via Heterogeneously Catalyzed Continuous-Flow Processes. Ph.D. Thesis, Technische Universität Berlin, Berlin, Germany, 1 October 2019.

40. Luo, J.; Yu, J.; Gorte, R.J.; Mahmoud, E.; Vlachos, D.G.; Smith, M.A. The effect of oxide acidity on HMF etherification. *Catal. Sci. Technol.* **2014**, *4*, 3074–3081. [[CrossRef](#)]
41. Lanzafame, P.; Papanikolaou, G.; Perathoner, S.; Centi, G.; Migliori, M.; Catizzone, E.; Aloise, A.; Giordano, G. Direct versus acetalization routes in the reaction network of catalytic HMF etherification. *Catal. Sci. Technol.* **2018**, *8*, 1304–1313. [[CrossRef](#)]
42. Raveendra, G.; Rajasekhar, A.; Srinivas, M.; Prasad, P.S.S.; Lingaiah, N. Selective etherification of hydroxymethylfurfural to biofuel additives over Cs containing silicotungstic acid catalysts. *Appl. Catal. A Gen.* **2016**, *520*, 105–113. [[CrossRef](#)]



© 2020 by the authors. Licensee MDPI, Basel, Switzerland. This article is an open access article distributed under the terms and conditions of the Creative Commons Attribution (CC BY) license (<http://creativecommons.org/licenses/by/4.0/>).